A New $^{1}_{\infty}[Ni_7]$ Cluster in $LaNi_7In_6$ and Distorted *bcc* Indium Cubes in $LaNiIn_4$

Yaroslav M. Kalychak,[b] Vasyl′ I. Zaremba,[b] Yaroslav V. Galadzhun,[b] Khrystyna Yu. Miliyanchuk,[b] Rolf-Dieter Hoffmann,[a] and Rainer Pöttgen*[a]

Abstract: $LaNiIn_4$ and $LaNi_7In_6$ were prepared by reaction of the elements in an arc melting furnace and subsequent annealing at 870 K for five weeks. Both compounds were investigated by X-ray diffraction on powders and single crystals and the structures were refined from single-crystal data: *Cmcm*, $a = 448.2(1)$, $b = 1689.5(4)$, $c = 722.1(1)$ pm, $wR2 = 0.0340$, 472 F^2 values, 24 variables for $LaNiIn_4$, and *Ibam*, $a = 806.6(2)$, $b = 924.8(2)$, $c = 1246.5(2)$ pm, $wR2 = 0.0681$, 726 F^2 values and 40 variables for $LaNi_7In_6$. $LaNiIn_4$ adopts the $YNiAl_4$-type structure. The nickel and indium atoms form a three-dimensional infinite $[NiIn_4]$ polyanion in which the lanthanum atoms fill distorted hexagonal channels. No Ni–Ni contacts occur. The indium substructure consists of distorted *bcc*-like indium cubes. $La-Ni_7In_6$ crystallizes with a peculiar new structure type. The nickel atoms build a $^{1}_{\infty}[Ni_7]$ cluster unit with Ni–Ni distances ranging from 249 to 269 pm. The cluster units are enveloped by indium atoms. These larger units show an orthorhombic rod packing with the lanthanum atoms filling the space between the rods. Several nickel clusters in ternary rare earth metal nickel indides and the structural relations of the $LaNi_7In_6$ structure with the cubic $NaZn_{13}$ type are discussed.

Keywords: chemical bonding · indium · lanthanum · nickel · structure elucidation

Introduction

The ternary systems rare earth metal (RE)/nickel/indium have been intensively investigated in the last 25 years.[1] So far, more than 120 ternary intermetallic compounds $RE_xNi_yIn_z$ have been synthesized. These intermetallics crystallize with 20 different structure types.[1, 2] Besides the large structural variety, these compounds have attracted considerable interest due to their peculiar magnetic and electrical properties. In this context the representatives with cerium, europium, and ytterbium have been studied most intensively. Several of these compounds show valence instabilities or interesting magnetic ordering phenomena. Remarkable compounds are intermediate-valent CeNiIn,[3–5] the intermediate heavy-fermion system $Ce_5Ni_6In_{11}$,[6, 7] antiferromagnetic $EuNiIn_4$,[8, 9] or the valence-unstable ytterbium compounds $YbNi_4In$ and $YbNiIn_4$.[10]

The highest magnetic ordering temperatures in such systems occur for the gadolinium-based compounds. Recently the 93.5 K ferromagnet GdNiIn was reported.[11] Such gadolinium-based intermetallic compounds are of considerable interest because of their potential use as magnetic refrigeration materials.[12–14] Another interesting chemical property of these intermetallic compounds is their hydrogen-storage behavior. The indides LaNiIn, CeNiIn, and NdNiIn can reversibly absorb hydrogen at room temperature and pressures up to 100 bar, resulting in the intermetallic hydrides $LaNiInH_{2.0}$, $CeNiInH_{1.8}$, and $NdNiInH_{1.7}$.[15] In contrast, the RENiIn indides with the heavier rare earth elements do not form hydrides.

The formation of such indium compounds strongly depends on the annealing temperatures. Thus, careful examination of the phase diagrams is required to determine the phase equilibria. During a systematic study of the lanthanum/nickel/indium system, we have synthesized single crystals of $LaNiIn_4$[8] and the new indide $LaNi_7In_6$. The crystal structures of and chemical bonding in both compounds are reported herein.

Experimental Section

Synthesis: Starting materials for the preparation of $LaNiIn_4$ and $LaNi_7In_6$ were ingots of lanthanum (Johnson Matthey), nickel wire (Johnson Matthey), and indium tear drops (Johnson Matthey), all with stated

[a] Prof. Dr. R. Pöttgen,[+] Dr. R.-D. Hoffmann[+]
Department Chemie, Ludwig-Maximilians-Universität München
Butenandtstrasse 5-13 (Haus D)
81377 München (Germany)
E-mail: pottgen@uni-muenster.de

[b] Dr. Y. M. Kalychak, Dr. V. I. Zaremba, Y. V. Galadzhun, K. Yu. Miliyanchuk
Inorganic Chemistry Department
Ivan Franko National University of Lviv
Kyryla and Mephodiya Street 6, 79005 Lviv (Ukraine)
E-mail: vazar@franko.lviv.ua

[+] New address: Institut für Anorganische und Analytische Chemie der Universität Münster
Wilhelm-Klemm-Strasse 8
48149 Münster (Germany)

  0947-6539/01/0724-5343 $ 17.50+.50/0

purities better than 99.9%. The large lanthanum ingots were cut into small pieces under paraffin oil and subsequently washed with *n*-hexane. The paraffin oil and *n*-hexane were dried over sodium wire. The compact lanthanum pieces were stored in Schlenk tubes under argon prior to the reactions. Argon was purified over titanium sponge (900 K), silica gel, and molecular sieves.

In a first step the lanthanum pieces were arc-melted to buttons. This premelting procedure minimizes shattering during the strongly exothermic reactions with nickel and indium. The lanthanum buttons were subsequently mixed with the nickel wire and the indium pieces in the ideal 1:1:4 and 1:7:6 atomic ratios and arc-melted under an argon pressure of about 800 mbar. The resulting buttons were turned over and remelted at least three times to achieve homogeneity. The total weight losses during the arc-melting procedures were all less than 0.5 wt%. Finally, fragments of the melted ingots were enclosed in evacuated silica tubes and annealed at 870 K for five weeks. The two indium compounds are stable in moist air for months. They are light gray in polycrystalline form. The single crystals exhibit metallic lustre.

X-ray investigations: The purity of the samples was checked through X-ray powder patterns (Dron-3M powder diffractometer, $Fe_{K\alpha}$ radiation) using 5N silicon ($a = 543.07$ pm) as an internal standard. The orthorhombic lattice parameters (see Table 1) were obtained from least-squares fits of the powder data. To ensure correct indexing the observed patterns were compared with calculated ones,[16] taking the atomic positions from the structure refinements. In both cases the lattice parameters determined from powder patterns and from single-crystal data agreed well. For $LaNiIn_4$ we observed also good agreement with the previously reported lattice parameters.[8]

Besides the $LaNi_7In_6$ sample, we also refined the lattice parameters originating from two additional samples: $a = 804.7(5)$, $b = 925.6(4)$, $c = 1246.1(6)$ pm, $V = 0.9281$ nm^3 for the starting composition 7.2 La:52.8 Ni:40 In and $a = 807.2(2)$, $b = 925.8(3)$, $c = 1247.8(3)$ pm, $V = 0.9325$ nm^3 for the starting composition 10 La:45 Ni:45 In. Within the combined standard deviations the differences in the cell volumes are not significant despite the fact that the single-crystal investigation indeed showed a mixed In/Ni occupancy for one indium position. This reflects a very small range of homogeneity.

Single-crystal intensity data of $LaNiIn_4$ were collected at room temperature by using a four-circle diffractometer (CAD4) with graphite-monochromated $Mo_{K\alpha}$ radiation (0.71073 pm) and a scintillation counter with pulse height discrimination. The scans were performed in the $\omega/2\theta$ mode. An empirical absorption correction was applied on the basis of psi-scan data. Intensity data of $LaNi_7In_6$ were collected by use of a Stoe image plate system (IPDS) with graphite-monochromated $Mo_{K\alpha}$ radiation in the oscillation mode. A numerical absorption correction was applied to these data. Crystallographic data and experimental details for both data collections are listed in Table 1.

Table 1. Crystal data and structure refinements for $LaNiIn_4$ and $LaNi_7In_6$.

empirical formula	$LaNiIn_4$	$LaNi_7In_6$
molar mass [g mol^{-1}]	656.90	1218.88
crystal system	orthorhombic	orthorhombic
lattice parameters		
a [pm]	448.2(1)	806.6(2)
b [pm]	1689.5(4)	924.8(2)
c [pm]	722.1(1)	1246.5(2)
V [nm^3]	0.5468	0.9298
space group	*Cmcm* (No. 63)	*Ibam* (No. 72)
Pearson symbol	oC24	oI56
Z	4	4
ρ_{calcd} [g cm^{-3}]	7.98	8.71
crystal size [μm^3]	$20 \times 20 \times 100$	$30 \times 30 \times 90$
transmission ratio (max/min)	1.47	1.77
μ [mm^{-1}]	27.4	32.6
$F(000)$	1124	2158
detector distance [mm]	–	50
exposure time [min]	–	4
φ range [°]; increment [°]	–	0–180; 1.4
profile/pixel	–	9–21
θ range for data collection [°]	2–30	2–31
range in *hkl*	$-6 \le h \le 4$, ± 23, $+10$	± 11, ± 13, ± 16
total no. reflections	1512	4627
independent reflections	472 ($R_{int} = 0.0305$)	726 ($R_{int} = 0.0603$)
reflections with $I > 2\sigma(I)$	423 ($R_{sigma} = 0.0253$)	617 ($R_{sigma} = 0.0359$)
data/parameters	472/24	726/40
goodness-of-fit on F^2	1.215	1.013
final R indices [$I > 2\sigma(I)$]		
$R1$	0.0192	0.0294
$wR2$	0.0328	0.0655
R indices (all data)		
$R1$	0.0243	0.0385
$wR2$	0.0340	0.0681
extinction coefficient	0.00200(9)	0.00052(8)
largest diff. peak and hole [e Å^{-3}]	0.85 and -1.73	2.01 and -3.04

Electronic structure calculations: Three-dimensional semiempirical band structure calculations for $LaNi_7In_6$ were based on an extended Hückel Hamiltonian.[17, 18] All exchange integrals, orbital exponents, and weighting coefficients were taken from a previous work on La_2Ni_2In.[19] Charge iterations have been carried out. The eigenvalue problem was solved in reciprocal space at 64 k points within the irreducible wedge of the Brillouin zone by using the YAeHMOP code.[20]

Results and Discussion

Structure refinements: Irregularly shaped single crystals of $LaNiIn_4$ and $LaNi_7In_6$ were isolated from the annealed samples by mechanical fragmentation and were examined by Buerger precession photographs to establish both symmetry and suitability for intensity data collection. The isotypy of $LaNiIn_4$ with the $YNiAl_4$ type[21] (space group *Cmcm*) was already evident from the powder pattern. A careful examination of the $LaNi_7In_6$ data set revealed a body-centered orthorhombic cell, and the extinction conditions were compatible with space group *Ibam*. Further crystallographic data are listed in Table 1.

Abstract in German: *$LaNiIn_4$ und $LaNi_7In_6$ wurden durch Reaktionen der Elemente in einem Lichtbogenofen und anschließendes fünfwöchiges Tempern bei 870 K synthetisiert. Beide Verbindungen wurden über Röntgen-Beugungsexperimente an Pulvern und Einkristallen untersucht und die Strukturen anhand von Einkristall-Diffraktometerdaten verfeinert: Cmcm, $a = 448.2(1)$, $b = 1689.5(4)$, $c = 722.1(1)$ pm, $wR2 = 0.0340$, 472 F^2-Werte, 24 Variable für $LaNiIn_4$ und Ibam, $a = 806.6(2)$, $b = 924.8(2)$, $c = 1246.5(2)$ pm, $wR2 = 0.0681$, 726 F^2-Werte und 40 Variable für $LaNi_7In_6$. $LaNiIn_4$ kristallisiert im $YNiAl_4$ Typ. Die Nickel- und Indiumatome bilden ein dreidimensionales $[NiIn_4]$-Polyanion ohne Ni-Ni-Kontakte, in dem die Lanthanatome verzerrte hexagonale Kanäle besetzen. Die Indium-Teilstruktur besteht aus verzerrten, bcc-ähnlichen Würfeln. $LaNi_7In_6$ kristallisiert mit einem neuen Strukturtyp. Die Nickelatome bilden $^1_\infty[Ni_7]$ Clusterstränge mit Ni-Ni-Abständen von 249 bis 269 pm. Diese Clusterstränge werden von den Indiumatomen umhüllt und bilden eine orthorhombische Stabpackung wobei die Lanthanatome den Platz zwischen den Stäben einnehmen. Die unterschiedlichen Nickelcluster in ternären Seltenerdmetall-Nickel-Indiden und die strukturelle Verwandtschaft der $LaNi_7In_6$ Struktur mit dem kubischen $NaZn_{13}$-Typ werden diskutiert.*

0947-6539/01/0724-5344 $ 17.50+.50/0 *Chem. Eur. J.* **2001**, *7*, No. 24

The atomic parameters of $EuNiIn_4$[9] were taken as starting values for $LaNiIn_4$, while those for $LaNi_7In_6$ were deduced from an automatic interpretation of data obtained by direct methods with SHELXS-97.[22] Both structures were successfully refined using SHELXL-97 (full-matrix least-squares on F^2)[23] with anisotropic atomic displacement parameters for all atoms. As a check for the correct composition, the occupancy parameters were refined in a separate series of least-squares cycles. Full occupancy within two standard deviations was observed for most sites, except the In2 site in $LaNi_7In_6$ which showed an occupancy of only 92.6(5)%. A similar occupancy was also found for a second crystal of this compound. Such homogeneity ranges are often observed in RE-Ni-In intermetallic compounds.[1] For the final least-squares cycles this position was refined with a mixed In2/Ni4 occupancy which revealed 82% indium and 18% nickel, resulting in a composition $LaNi_{7.36}In_{5.64}$ for the investigated crystal. Final difference Fourier syntheses revealed no significant residual peaks (see Table 1). The positional parameters and interatomic distances of the two refinements are listed in Tables 2 and 3. Further details on the crystal structure investigations may be obtained from the Fachinformationszentrum Karlsruhe, 76344 Eggenstein-Leopoldshafen, Germany (fax: (+49) 7247-808-666; e-mail: crysdata@fiz-karlsruhe.de), on quoting the depository numbers CSD-411746 ($LaNiIn_4$) and CSD-411747 ($LaNi_7In_6$).

Table 2. Atomic coordinates and isotropic displacement parameters [pm^2] for $LaNiIn_4$ and $LaNi_7In_6$. U_{eq} is defined as one third of the trace of the orthogonalized U_{ij} tensor.

Atom	Occ.	Wyckoff position	x	y	z	U_{eq}
$LaNiIn_4$ (space group *Cmcm*)						
La		4*c*	0	0.11786(3)	1/4	83(1)
Ni		4*c*	0	0.77329(6)	1/4	91(2)
In1		8*f*	0	0.31135(2)	0.04940(6)	85(1)
In2		4*c*	0	0.92409(4)	1/4	112(1)
In3		4*b*	0	1/2	0	123(1)
$LaNi_7In_6$ (space group *Ibam*)						
La		4*a*	0	0	1/4	123(2)
Ni1		4*d*	0	1/2	0	75(4)
Ni2		8*j*	0.0758(1)	0.2388(1)	0	77(3)
Ni3		16*k*	0.6245(1)	0.08896(9)	0.17140(8)	69(2)
In1		16*k*	0.17351(5)	0.69254(5)	0.13737(4)	92(2)
In2	0.820(5)	8*j*	0.17391(8)	0.95635(7)	0	79(3)
Ni4	0.180(5)	8*j*	0.17391(8)	0.95635(7)	0	79(3)

Crystal chemistry and chemical bonding: $LaNiIn_4$ is the most indium-rich compound in the ternary system lanthanum/nickel/indium. Although X-ray powder data have been reported earlier,[8] we have now refined the structure on the basis of single-crystal data.

$LaNiIn_4$ adopts the $YNiAl_4$-type structure.[21] Since the crystal chemistry of these intermetallic compounds has already been discussed in detail from a geometrical point of view,[8, 9, 24] we focus here on chemical bonding in $LaNiIn_4$. Figure 1 shows a view of the $LaNiIn_4$ structure approximately along the *x* axis. The nickel and indium atoms build a three-dimensional $[NiIn_4]$ polyanionic network with Ni–In distances ranging from 255 to 275 pm. The average Ni–In distance of 267 pm is in good agreement with the sum of Pauling's single bond radii[25] of 265 pm for nickel and indium. No Ni–Ni contacts occur. The three crystallographically different indium atoms build distorted *bcc*-like cubes. The various In–In contacts within and between these cubes cover a large range from 290 to 361 pm. Notably, the shortest In–In distance of 290 pm is significantly shorter than in tetragonal body-centered indium ($a = 325.2$, $c = 494.7$ pm),[26] in which each

Table 3. Interatomic distances [pm], calculated with the lattice parameters taken from X-ray powder data of $LaNiIn_4$ and $LaNi_7In_6$. All distances within the first coordination sphere are listed. Standard deviations are all equal or less than 0.2 pm. Note, the In2 position of $LaNi_7In_6$ has a mixed occupancy of 82% In and 18% Ni.

	$LaNiIn_4$				$LaNi_7In_6$				$LaNi_7In_6$			
La:	1	In2	327.4	La:	4	Ni3	328.8	In1:	1	Ni3	259.9
	4	In1	333.6		4	In2	344.1		1	Ni3	262.2
	2	Ni	345.2		4	In1	346.6		1	Ni3	263.0
	4	In3	349.9		4	In1	347.5		1	Ni3	266.7
	2	In1	357.6		4	Ni2	386.8		1	Ni2	268.4
	2	In2	367.9						1	Ni2	271.6
	2	Ni	405.2	Ni1:	2	Ni2	249.2		1	Ni1	283.9
	2	La	448.2		4	Ni3	250.0		1	In2	298.1
					2	In2	266.1		1	In2	303.6
Ni:	1	In2	254.8		4	In1	283.9		1	In1	324.6
	2	In1	259.2						1	In1	342.5
	4	In1	274.5	Ni2:	1	Ni1	249.2		1	La	346.6
	2	La	345.2		2	In1	268.4		1	La	347.5
	2	La	405.2		2	Ni3	269.4				
					1	In2	270.4	In2:	1	Ni1	266.1
In1:	1	Ni	259.2		2	In1	271.6		1	Ni2	270.4
	2	Ni	274.5		1	In2	272.9		2	Ni3	271.8
	1	In1	289.7		1	In2	285.0		1	Ni2	272.9
	2	In1	313.5		2	La	386.8		1	Ni2	285.0
	1	In3	320.7						1	In2	291.9
	2	In2	327.9	Ni3:	1	Ni1	250.0		2	In1	298.1
	2	La	333.6		1	Ni3	255.9		2	In1	303.6
	1	La	357.6		1	Ni3	259.6		2	La	344.1
					1	In1	259.9				
In2:	1	Ni	254.8		1	In1	262.2				
	4	In3	315.1		1	In1	263.0				
	1	La	327.4		1	In1	266.7				
	4	In1	327.9		1	Ni2	269.4				
	2	La	367.9		1	In2	271.8				
					1	Ni3	280.6				
In3:	4	In2	315.1		1	La	328.8				
	2	In1	320.7								
	4	La	349.9								
	2	In3	361.1								

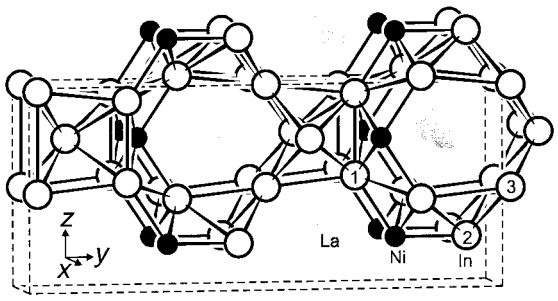

Figure 1. Crystal structure of $LaNiIn_4$ viewed along approximately the *x* axis. The lanthanum, nickel, and indium atoms are drawn as gray, black, and open circles, respectively. The three-dimensional $[NiIn_4]$ polyanion is emphasized. A *bcc*-like cube of indium atoms is outlined in the upper left-hand corner of the unit cell.

indium atom has four nearest neighbors at 325 pm and eight further neighbors at 338 pm.

The common structural motif of such indium-rich ternary intermetallics are distorted *bcc*-like indium cubes. The various types of these cubes have been presented in two previous papers.[27, 28] Earlier, chemical bonding was investigated by extended Hückel calculations for $CaPdIn_4$.[27] These semi-empirical calculations revealed a net Mulliken charge of $+1.69$ for calcium and of -0.93 for palladium as a consequence of d-band filling. The strongest bonding interactions were found for the Pd–In and In–In contacts. In view of the electropositive character of calcium and the strongly bonding Pd–In and In–In interactions, the formulation $Ca^{2+}[PdIn_4]^{2-}$ is adequate, emphasizing the essentially covalently bonded $[PdIn_4]$ polyanion. Since lanthanum and nickel have electronegativities similar to calcium and palladium,[29] the model of chemical bonding in $CaPdIn_4$ may safely be applied to $LaNiIn_4$.

$LaNi_7In_6$ is the thirteenth indide with known crystal structure in the system lanthanum/nickel/indium.[1] It crystallizes with a new structure type. Within the structure we find three crystallographically different nickel sites with Ni–Ni distances ranging from 249 to 269 pm with an average of 254 pm. In view of the Ni–Ni distance of 249 pm in *fcc* nickel,[26] we can assume a significant degree of Ni–Ni bonding.

Together, the nickel atoms build a one-dimensional $[Ni_7]$ cluster chain. A section of this cluster unit is presented in Figure 2. This chain is composed of condensed distorted Ni_4 tetrahedra and linear Ni_3 chains. To our knowledge, this is a new motif in the crystal chemistry of such cluster compounds. The one-dimensional $[Ni_7]$ chains are surrounded by indium atoms at Ni–In distances ranging from 260 to 285 pm. Also the average Ni–In distance of 272 pm is in good agreement with the sum of Pauling's single bond radii[25] (see above). The clusters are arranged in the form of an orthorhombic rod, packing as shown in Figure 3. The lanthanum atoms fill the space between the rods. In view of Pauling's electronegativities[29] of 1.1, 1.91, and 1.78, for lanthanum, nickel, and indium, respectively, the lanthanum atoms have most likely transferred their valence electrons to the nickel and indium atoms. In emphasizing the Ni–Ni and Ni–In bonding, the electron counting can, to a first approximation, be written as $La^{3+}[Ni_7In_6]^{3-}$. This structural arrangement is very similar to that in oxomolybdates like $NaMo_4O_6$,[30] where the sodium atoms fill channels between the chains of edge-sharing Mo_6O_{12}-type clusters. One significant difference, however, is that in $LaNi_7In_6$ also weak La–Ni and La–In contacts exist and that the In2 position is partially occupied by nickel. This seems to weaken the cluster concept, but is still tolerable in an intermetallic compound.

Recent investigations of the ternary system Eu/Ni/In revealed orthorhombic compounds $EuNi_{7+x}In_{6-x}$.[31] In contrast to the lanthanum compound, the europium indide shows a pronounced homogeneity range approximately from 34 to 43 atom-% indium. Detailed studies of the structures and properties of these samples are currently in progress.

Chemical bonding in $LaNi_7In_6$ was investigated by semi-empirical extended Hückel calculations. The density-of-states

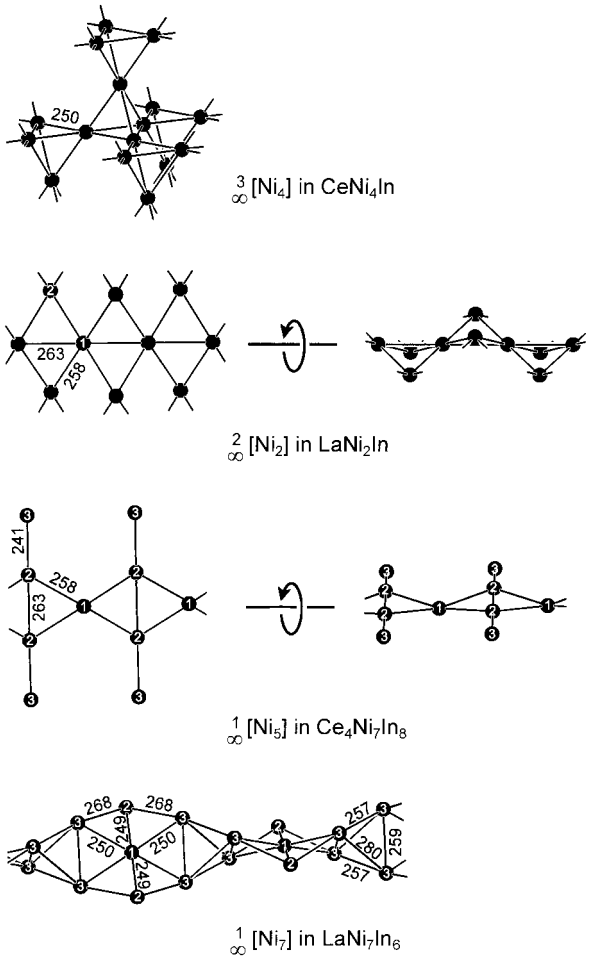

Figure 2. Sections of the cluster units in the structures of $CeNi_4In$, $LaNi_2In$, $Ce_4Ni_7In_8$, and $LaNi_7In_6$. Relevant interatomic distances are indicated in pm.

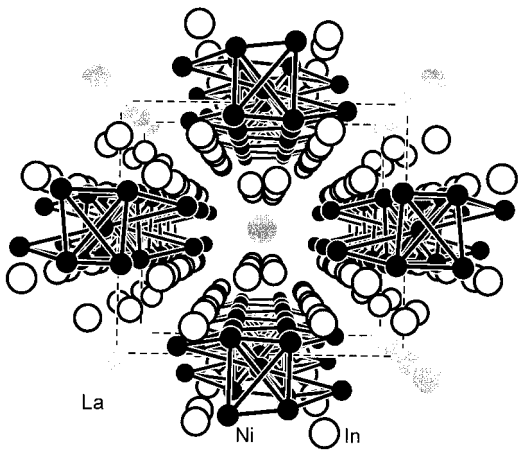

Figure 3. Perspective view of the $LaNi_7In_6$ structure along the z axis. The one-dimensional $[Ni_7]$ cluster chain is emphasized. The lanthanum and indium atoms are drawn as gray and open circles, respectively.

(DOS) curve is presented in Figure 4. The nickel d-block stays sharply localized at around -18 eV and the broadened indium states mix in from -18 eV up to and beyond the Fermi level. The gross Mulliken charges are La $+1.81$, Ni -0.94, and In $+0.80$. It should be noted that the electronic structure calculations were performed for the ideal composition

0947-6539/01/0724-5346 $ 17.50+.50/0 *Chem. Eur. J.* **2001**, *7*, No. 24

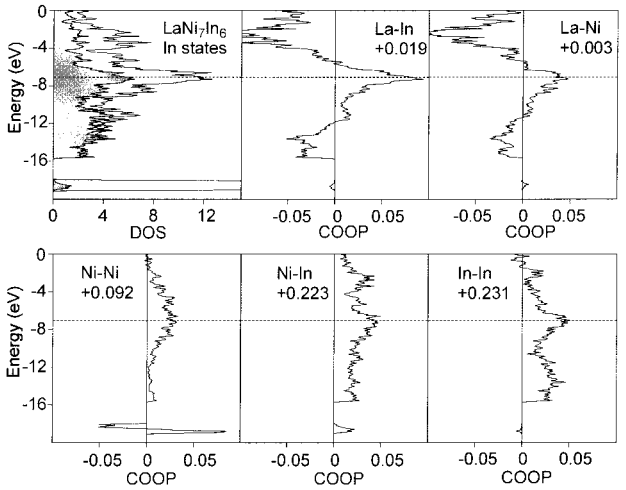

Figure 4. Total and projected DOS curve for $LaNi_7In_6$ (upper left-hand drawing). The indium contributions are emphasized in grey. Also the COOP curves for the La–In, La–Ni, Ni–Ni, Ni–In, and In–In interactions with the integrated values of the overlap populations are shown.

$LaNi_7In_6$. Since the homogeneity range is very small, this will hardly affect the principle statement concerning the chemical bonding.

Semiempirical crystal orbital overlap population (COOP) allows a more quantitative bond analysis. The Ni–Ni COOP curve (lower left-hand part of Figure 4) shows that both Ni–Ni bonding and antibonding states are filled, a result which is not unusual given that it is formally a closed-shell interaction. This is also expressed in a relative low overlap population (OP) value of +0.092. The various Ni–In (260–285 pm) and In–In (292–343 pm) contacts are significantly bonding. The Ni–In (+0.223) and In–In (+0.231) OP values are the highest in the $LaNi_7In_6$ structure. The La–Ni and La–In bonding with OP +0.019 and +0.003, respectively, play a very subordinate role (upper right-hand part of Figure 4). The small OPs and the course of the Mulliken charges fully justify the formulation $La^{3+}[Ni_7In_6]^{3-}$ discussed above.

Turning now to the one-dimensional $[Ni_7]$ cluster chain. Within the large series of rare earth metal nickel indides only few show extended nickel clusters. Besides some structures with Ni_2 pairs only the structures of $CeNi_4In$, $LaNi_2In$, $Ce_4Ni_7In_8$, and $LaNi_7In_6$ contain larger cluster units as presented in Figure 2. The cluster with the highest symmetry occurs in $CeNi_4In$[32] where the nickel atoms form a three-dimensional network of corner-sharing tetrahedra with Ni–Ni distances of 250 pm. In $LaNi_2In$[33] the nickel cluster is two-dimensional (Figure 2). Each nickel atom has six nickel neighbors like in a close-packed layer. However, these layers show strong puckering in $LaNi_2In$. The Ni–Ni distances of 258 and 263 pm are slightly longer than those in $CeNi_4In$. The nickel network is one-dimensional in $Ce_4Ni_7In_8$.[34] It is composed of Ni_4 chains (Ni–Ni distances 241 and 263 pm) which are interconnected through further nickel atoms at 258 pm. The one-dimensional $[Ni_7]$ cluster chain in $LaNi_7In_6$, however, is more complex. The cluster units presented in Figure 2 are only sections of the respective structures. In most cases they are surrounded by indium atoms and the rare earth atoms fill the space between the indium-enveloped cluster units.

Finally we emphasize that the structure of $LaNi_7In_6$ can be considered as a ternary ordered derivative of the cubic $NaZn_{13}$ type (Pearson code *cF*112, space group $Fm\bar{3}c$, $a=$ 1228.36 pm).[35] From a geometrical point of view, the $NaZn_{13}$ structure is built up from a packing of sodium atoms and isolated $[Zn1Zn2_{12}]$ icosahedra in a CsCl-like manner (Figure 5).[36] A very similar packing is found for the structures of $CeNi_{8.5}Si_{4.5}$ (*tI*56, space group *I*4/*mcm*, $a=785.7$, $c=$ 1150.3 pm)[37] and $LaNi_7In_6$ (*oI*56, space group *Ibam*, $a=$ 806.6, $b=924.8$, $c=1246.5$ pm). However, the icosahedra are formed by nickel and silicon or nickel and indium atoms, leading to significant structural distortions: the $CeNi_{8.5}Si_{4.5}$ structure is tetragonal and $LaNi_7In_6$ is orthorhombic.

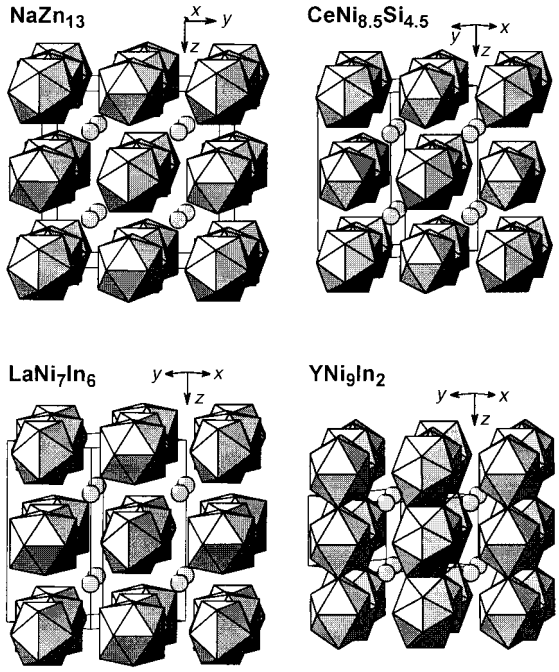

Figure 5. The crystal structures of $NaZn_{13}$, $CeNi_{8.5}Si_{4.5}$, $LaNi_7In_6$, and YNi_9In_2. The packing of alkali and rare earth metal atoms and the icosahedral units are emphasized. Shaded atoms are Na, Ce, La, or Y. In $NaZn_{13}$, $CeNi_{8.5}Si_{4.5}$, and $LaNi_7In_6$ the icosahedra are isolated, but they are condensed along edges along the *z* axis in YNi_9In_2. For details see text.

The structures of $NaZn_{13}$, $CeNi_{8.5}Si_{4.5}$, and $LaNi_7In_6$ are directly related through a group–subgroup relation as presented in the concise and compact Bärnighausen formalism[38, 39] in Figure 6. The space group symmetry is lowered from $F4/m\bar{3}2/c$ to $I4/m2/c2/m$ by a *translationengleiche* reduction of index 3 (t3). This way the 96-fold Zn2 position of $NaZn_{13}$ splits into three 16-fold positions in $CeNi_{8.5}Si_{4.5}$. Further symmetry reduction (t2) to the orthorhombic space group $I2/b2/a2/m$ ($LaNi_7In_6$) results in a further splitting of a 16-fold position into two eightfold positions. Since both symmetry reductions are *translationengleich*, multiple twinning might occur, however, this was luckily not the case for $LaNi_7In_6$.

The degree of the distortions from cubic symmetry seems to be closely related to the difference in size of the atoms which

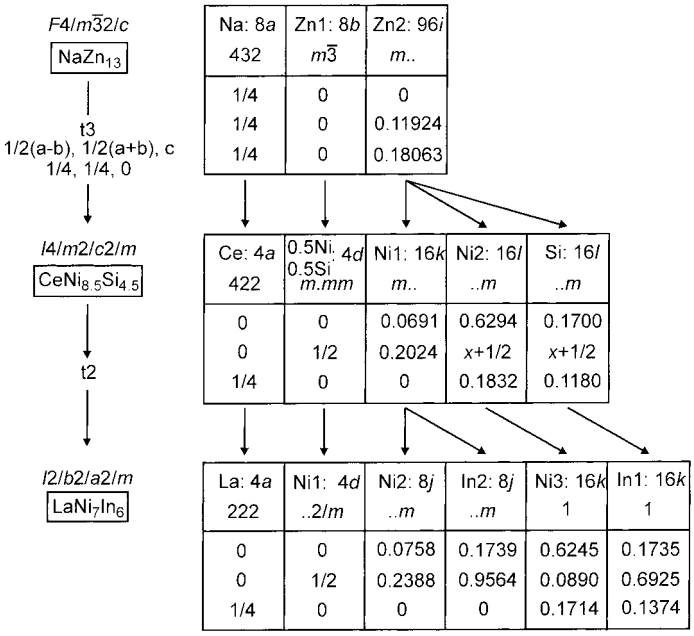

Figure 6. Group–subgroup relation in the Bärnighausen formalism[38, 39] for the structures of $NaZn_{13}$, $CeNi_{8.5}Si_{4.5}$, and $LaNi_7In_6$. The indices of the *translationengleiche* (t) transitions, the unit cell transformations with origin shifts and the evolution of the atomic parameters are given.

occupy the two crystallographically different zinc sites. In $CeNi_{8.5}Si_{4.5}$ nickel (115 pm) and silicon (117 pm) differ only slighly in their metallic single bond radii.[25] Consequently we observe only a small tetragonal distortion of the cubic cell with a c/a ratio (1.464) close to $\sqrt{2}$. In contrast, the nickel (115 pm) and indium (150 pm) atoms in $LaNi_7In_6$ differ significantly in size. Therefore clustering of the smaller nickel atoms occurs, leading to c/b and c/a ratios of 1.348 and 1.545, respectively, which significantly deviate from the ideal ratio of $\sqrt{2}$.

$CeNi_{8.5}Si_{4.5}$ and $LaNi_7In_6$ are closely related to the $Ce(Mn/Ni)_{11}$ structure.[40] For the indium systems its superstructure with ordered transition metal and indium positions, the YNi_9In_2 type (*tP*24, *P*4/*mbm*, $a = 822.2$, $c = 482.7$ pm) is typical.[41] It contains similar icosahedral groups. These icosahedra, however, are not isolated. They are condensed through common edges along the z axis, leading to a change in composition from 1:13 to 1:11.

Projections of the four structures are displayed in Figure 7. The unit cell of the tetragonal (t) $CeNi_{8.5}Si_{4.5}$ structure is derived from the cubic (c) $NaZn_{13}$ type through the relation $a_t \approx 1/2a_c - 1/2b_c$, $b_t \approx 1/2a_c + 1/2b_c$, $c_t \approx c_c$. The c lattice parameter of the YNi_9In_2 structure is approximately $1/2c_c$. $CeNi_{8.5}Si_{4.5}$ and $LaNi_7In_6$ consist of two YNi_9In_2 cells along the

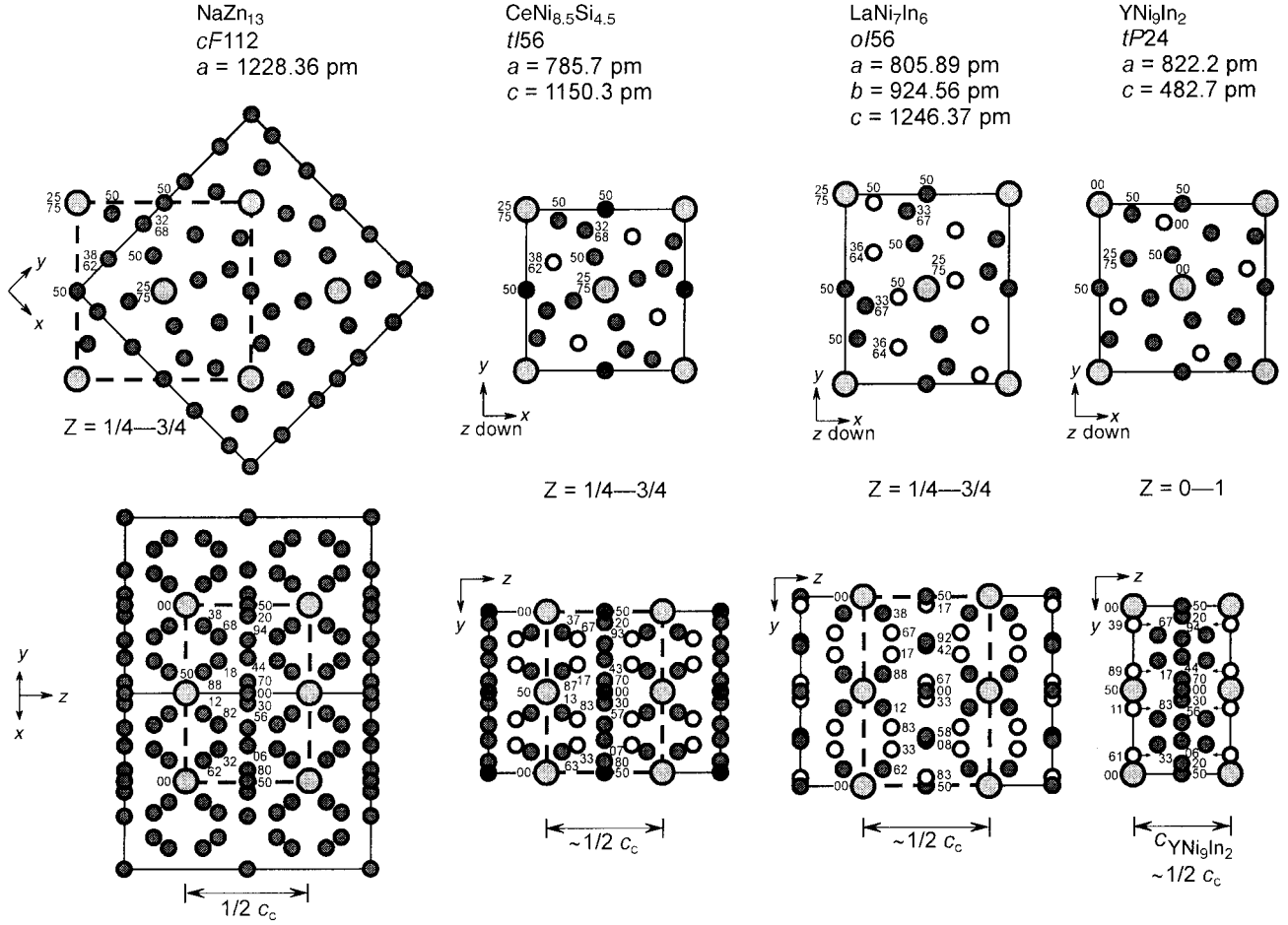

Figure 7. Projections of the cubic $NaZn_{13}$ type structure and its ternary derivatives: tetragonally distorted $CeNi_{8.5}Si_{4.5}$ and orthorhombically distorted $LaNi_7In_6$. For comparison, also the YNi_9In_2 structure is shown. The Pearson code, the unit cell parameters and the heights of the atoms are indicated for each structure. Large gray circles: Na, La, Ce, and Y; small gray circles: Zn and Ni atoms; small white circles: Si and In atoms; dark gray circles: mixed Ni/Si sites. For details see text.

0947-6539/01/0724-5348 $ 17.50+.50/0 *Chem. Eur. J.* **2001**, *7*, No. 24

[001] direction. The change in composition from 1:11 (YNi_9In_2) to 1:13 ($CeNi_{8.5}Si_{4.5}$ and $LaNi_7In_6$) is due to the different site multiplicity of the 4*g* site in YNi_9In_2 to the 16*k* site in $CeNi_{8.5}Si_{4.5}$ and $LaNi_7In_6$. The shift of the indium atoms is emphasized by small arrows in the lower right-hand drawing of Figure 7.

Pearson's Handbook[42] lists several aluminides and silicides with compositions close to RET_7Al_6 and RET_7Si_6 with the $NaZn_{13}$ type structure. A description of these structures, however, is only possible with statistically occupied *T*/Al or *T*/Si sites. An ordering of the transition metal and aluminium(silicon) atoms is possible in the $NaZn_{13}$ superstructures $CeNi_{8.5}Si_{4.5}$ and $LaNi_7In_6$. Nevertheless, careful examination of the intensities and peak splitting due to possible twinning should be considered for $NaZn_{13}$-related structures.

Summing up, we have refined the structures of $LaNiIn_4$ and $LaNi_7In_6$, both with distincly different structural motifs. Indium-rich $LaNiIn_4$ contains distorted *bcc*-like indium cubes and the nickel atoms in $LaNi_7In_6$ build a one-dimensional $[Ni_7]$ cluster chain. Chemical bonding analyses are in agreement with the formulæ $La^{3+}[NiIn_4]^{3-}$ and $La^{3+}[Ni_7In_6]^{3-}$. The lanthanum atoms are located in distorted hexagonal channels in $LaNiIn_4$, while they separate one-dimensional $[Ni_7In_6]$ rods in $LaNi_7In_6$.

Acknowledgements

We are indebted to Dr. H. Piotrowski for collecting the IPDS data. This work was financially supported by the Fonds der Chemischen Industrie and the Deutsche Forschungsgemeinschaft.

[1] Ya. M. Kalychak, *J. Alloys Compd*. **1997**, *262–263*, 341.
[2] V. I. Zaremba, Ya. M. Kalychak, V. P. Dubenskiy, R.-D. Hoffmann, R. Pöttgen, *J. Solid State Chem*. **2000**, *152*, 560.
[3] K. Satoh, T. Fujita, Y. Maeno, Y. Uwatoko, H. Fujii, *J. Phys. Soc. Jpn*. **1990**, *59*, 692.
[4] M. Kurisu, T. Takabatake, H. Fujii, *J. Magn. Magn. Mater*. **1990**, *90&91*, 469.
[5] H. Fujii, T. Takabatake, V. Andoh, *J. Alloys Compd*. **1992**, *181*, 111.
[6] Ya. M. Kalychak, P. Yu. Zavalii, V. M. Baranyak, O. V. Dmytrakh, O. I. Bodak, *Sov. Phys. Crystallogr*. **1987**, *32*, 600 (*Kristallografiya* **1987**, *32*, 1021).
[7] J. Tang, K. A. Gschneidner, Jr., S. J. White, M. R. Roser, T. J. Goodwin, L. R. Corrucini, *Phys. Rev. B* **1995**, *52*, 7328.
[8] Ya. M. Kalychak, V. M. Baranyak, V. I. Zaremba, P. Yu. Zavalii, O. V. Dmytrakh, V. A. Bruskov, *Sov. Phys. Crystallogr*. **1988**, *33*, 602.
[9] R. Pöttgen, R. Müllmann, B. D. Mosel, H. Eckert, *J. Mater. Chem*. **1996**, *6*, 801.
[10] M. D. Koterlin, B. S. Morokhivskii, I. D. Shcherba, Ya. M. Kalychak, *Phys. Solid State* **1999**, *41*, 1759.
[11] F. Merlo, M. L. Fornasini, S. Cirafici, F. Canepa, *J. Alloys Compd*. **1998**, *267*, L12.
[12] V. K. Pecharsky, K. A. Gschneidner Jr., *Appl. Phys. Lett*. **1997**, *70*, 3299.
[13] V. K. Pecharsky, K. A. Gschneidner Jr., *Adv. Cryo. Eng*. **1998**, *43*, 1729.
[14] K. A. Gschneidner Jr., V. K. Pecharsky, *Annu. Rev. Mater. Sci*. **2000**, *30*, 387.
[15] I. I. Bulyk, V. A. Yartys, R. V. Denys, Ya. M. Kalychak, I. R. Harris, *J. Alloys Compd*. **1999**, *284*, 256.
[16] K. Yvon, W. Jeitschko, E. Parthé, *J. Appl. Crystallogr*. **1977**, *10*, 73.
[17] R. Hoffmann, *J. Chem. Phys*. **1963**, *39*, 1397.
[18] R. Hoffmann, *Solids and Surfaces: A Chemist's View of Bonding in Extended Structures*, VCH, Weinheim, **1988**.
[19] R.-D. Hoffmann, A. Fugmann, U. Ch. Rodewald, R. Pöttgen, *Z. Anorg. Allg. Chem*. **2000**, *626*, 1733.
[20] G. A. Landrum, *YAeHMOP*, Version 2.0, **1997**; available on: http://overlap.chem.cornell.edu:8080/yaehmop.html.
[21] R. M. Rykhal', O. S. Zarechnyuk, Ya. P. Yarmolyuk, *Sov. Phys. Crystallogr*. **1972**, *17*, 453.
[22] G. M. Sheldrick, SHELXS-97, *Program for Crystal Structure Solution*, University of Göttingen, Germany, **1997**.
[23] G. M. Sheldrick, SHELXL-97, *Program for Crystal Structure Refinement*, University of Göttingen, Germany, **1997**.
[24] R. Pöttgen, *J. Mater. Chem*. **1995**, *5*, 769.
[25] L. Pauling, *The Nature of the Chemical Bond and the Structure of Molecules and Crystals*, Cornell University Press, Ithaca, NY, **1960**.
[26] J. Donohue, *The Structures of the Elements*, Wiley, New York, **1974**.
[27] R.-D. Hoffmann, R. Pöttgen, *Chem. Eur. J*. **2000**, *6*, 600.
[28] R.-D. Hoffmann, R. Pöttgen, V. I. Zaremba, Ya. M. Kalychak, *Z. Naturforsch. B* **2000**, *55*, 834.
[29] J. Emsley, *The Elements*, Oxford University Press, 3rd ed., **1998**.
[30] A. Simon, "Metal-rich compounds" in *Solid State Chemistry: Compounds* (Eds.: A. K. Cheetham, P. Day), Clarendon Press, Oxford, **1992**.
[31] V. I. Zaremba, Ya. V. Galadzhun, Ya. M. Kalychak, R.-D. Hoffmann, R. Pöttgen, unpublished results.
[32] M. D. Koterlin, B. S. Morokhivskii, R. R. Kutyanskii, I. D. Shcherba, Ya. M. Kalychak, *Fiz. Tverd. Tela* **1998**, *40*, 7.
[33] Ya. M. Kalychak, V. I. Zaremba, *Kristallografiya* **1994**, *39*, 923.
[34] V. M. Baranyak, Ya. M. Kalychak, V. A. Bruskov, P. Yu. Zavalii, O. V. Dmytrakh, *Sov. Phys. Crystallogr*. **1988**, *33*, 353.
[35] D. P. Shoemaker, R. E. Marsh, F. J. Ewing, L. Pauling, *Acta Crystallogr*. **1952**, *5*, 637.
[36] P. I. Kryp'yakevitch, *The Structural Types of the Intermetallic Compounds*, Nauka, Moscow, **1977**.
[37] O. I. Bodak, *Kristallografiya*. **1979**, *24*, 1280.
[38] H. Bärnighausen, *Commun. Math. Chem*. **1980**, *9*, 139.
[39] H. Bärnighausen, U. Müller, *Symmetriebeziehungen zwischen den Raumgruppen als Hilfsmittel zur straffen Darstellung von Strukturzusammenhängen in der Kristallchemie*, University of Karlsruhe and University/GH Kassel, Germany, **1996**.
[40] Ya. M. Kalychak, L. G. Aksel'rud, Ya. P. Yarmolyuk, O. I. Bodak, E. I. Gladyshevskii, *Kristallografiya*. **1976**, *20*, 639.
[41] Ya. M. Kalychak, L. G. Aksel'rud, V. I. Zaremba, V. M. Baranyak, *Dop. AN URSSR*. **1984**, 37.
[42] P. Villars, L. D. Calvert, *Pearson's Handbook of Crystallographic Data for Intermetallic Phases*, 2nd ed, American Society for Metals, Materials Park, OH 44073, **1991**, and Desk Edition, **1997**.

Received: February 19, 2001
Revised: July 18, 2001 [F3082]